Single-Phase Heat Transfer and Pressure Drop of the Cooling of Water inside Smooth Tubes for Transitional Flow with Different Inlet Geometries (RP-1280)

J.A. Olivier **J.P. Meyer, PhD, PrEng**
Member ASHRAE

Received March 4, 2010; accepted March 22, 2010

This paper is based on findings resulting from ASHRAE Research Project RP-1280

Design constraints and energy requirements have often led to heat exchangers operating outside of their design parameters. These parameters often involve the exchanger operating in the transition region of flow. Adiabatic as well as diabatic experiments were conducted inside smooth tubes with diameters of 15.88 mm (5/8 in.) and 19.02 mm (3/4 in.). Four inlet profiles were investigated; hydrodynamically fully developed, square-edged, re-entrant, and bellmouth. The test fluid was water that was cooled, with Reynolds numbers ranging between 1000 and 20,000, Prandtl numbers between 4 and 6, and Grashof numbers in the order of 10^5. Adiabatic results showed that transition from laminar to turbulent flow was strongly dependent on the inlet profile, with transition being delayed to Reynolds numbers as high as 12,000, confirming results of previous studies. Diabatic heat transfer and friction factor results showed that transition was independent of the inlet, with transition occurring at a Reynolds number of approximately 2100. This was due to the secondary flow suppressing the disturbance of the inlets. Laminar heat transfer and friction factors were also substantially higher than when compared with their theoretical counterparts. This could also be attributed to secondary flows, confirming previously published results. A direct relationship between friction factor and heat transfer exists and is shown to predict 88% of the friction factor data to within 15%, with a mean absolute error of 8.7% when using well-known laminar and turbulent heat transfer correlations.

INTRODUCTION

It is accepted in literature that transition from laminar to turbulent flow inside tubes occurs at a Reynolds number of approximately 2300 (ASHRAE 2009). Although this is an accepted value, in reality, transition occurs in Reynolds numbers ranging from 2300 to 10,000 (Ghajar and Tam 1994). When designing heat exchangers, people are usually advised to remain outside of these limits due to the uncertainty and flow instability of this region. Large pressure variations are also encountered in this region, since the pressure gradient required to move the fluid in laminar and turbulent flow could vary by an order of magnitude.

Inlet profiles were found to have a profound influence on the transition Reynolds number. Nagendra (1973) found that the greater the disturbance, the earlier transition occurs. Ghajar and Madon (1992) performed an extensive study into the effect of three different types of inlets on the critical Reynolds number during isothermal, fully developed flow. The three types of inlets tested were square-edged (sudden contraction), re-entrant (tube-protruding, square-edged inlet),

J.A. Olivier is a postgraduate student and **J.P. Meyer** is a professor and head of the Department of Mechanical and Aeronautical Engineering at the University of Pretoria, Pretoria, South Africa.

and bellmouth (smooth, gradual contraction). It was found that transition from laminar to turbulent flow occurred at Reynolds numbers of 1980 to 2600 for the re-entrant, 2070 to 2840 for the square-edged, and 2125 to 3200 for the bellmouth inlet. A study performed by Smith (1960) indicated that transition occurred in the inlet–developing length of the tube and not in the fully developed Poiseuille region. This, combined with the work of Ghajar and Madon, showed that the inlet acts as a disturbance to the flow. The smoother the inlet, the more transition is delayed. Results published in later work by Tam and Ghajar (1997) showed transition to occur at different Reynolds numbers (much higher) than previous results. The transition for the re-entrant inlet started and ended at 2900 to 3500, at 3100 to 3700 for the square-edged, and at 5100 to 6100 for the bellmouth.

Heat transfer results by Ghajar and Tam (1994) also showed that transition varied from inlet to outlet. For the re-entrant inlet, it started and ended at a Reynolds number of 2000 and 6700, respectively, near the inlet of the tube (3 diameters from the inlet), and 2100 and 8500 near the exit (192 diameters from the inlet). For the square-edged inlet, these limits were 2400 to 7300 and 2500 to 8800, and for the bellmouth they were 3400 to 9400 and 3800 to 10,500. This variation from inlet to outlet, as explained by Ghajar and Tam (1991), is due to the variation in fluid properties. Since the tube was under a uniform heat flux boundary, the fluid was heated along the axial length, with the effect of the viscosity decreasing, and hence, an increase in Reynolds number while the mass flow rate remained the same. Correlations were developed to predict the critical Reynolds numbers for the different inlets. Further correlations were also developed to predict heat transfer in the transition region of flow.

To determine the effect of buoyancy forces—in the form of natural convection—have on transition, Mori et al. (1966) performed tests using air. After the settling chamber a series of disturbances in the form of rings were inserted, which generated turbulence. The tests with the disturbance revealed that as the Rayleigh number (accounting for buoyancy-induced secondary flows) was increased, the critical Reynolds number increased. The reason for this is that the secondary flow suppresses the turbulence being created by the disturbance. For tests with no disturbance, it was found that the critical Reynolds number decreased with an increase in Rayleigh number due to the secondary flow actually generating the turbulence. They observed that when the product of the Reynolds and Rayleigh number was large, the secondary flow caused the critical Reynolds numbers to approach the same value, whether the turbulence level at the entrance of the tube was high or low. Nagendra (1973) found similar findings while performing extensive transition regime tests.

Heat transfer also had an effect on the laminar friction factor, which increased with the amount of heat being added (Tam and Ghajar 1997). This effect was also observed by Nunner (1956). The increase (as much as 100%) was attributed to the buoyancy-induced secondary flows altering the velocity profile, which, in turn, influenced the shear stress at the tube wall.

The main objective of this paper is to report on newly obtained data on adiabatic and diabatic transitional heat transfer and pressure drop inside smooth horizontal tubes with various inlet geometries. Two tubes with different diameters were investigated, with the working fluid being water that was cooled, which is typical of water-chiller units. The boundary condition would then be close to that of a constant wall temperature, rather than a uniform heat flux, which is found in many research papers. The cooling of a fluid was shown to have different characteristics than a fluid being heated. This was shown by Petukhov et al. (1969) who developed a turbulent heat transfer correlation for both instances but found that the results for the fluid being cooled reacted differently to the heating data. It should also be noted that the effect of viscosity is also different. For the case where the fluid is being heated, the viscosity near the wall is lower than the bulk, while for a fluid being cooled, it is higher. Thus, higher shear stress at the wall can be expected for a cooling fluid, which could lead to higher pressure drops. Since water was used

for all the experiments, the Prandtl number remained relatively constant for all Reynolds numbers tested. This is unlike other work where a high Prandtl number fluid was used at low flow rates due to the limited range of the pumps and due to pressure drops being higher, improving their uncertainty during measurements. More details and other differences are given by Olivier (2009).

EXPERIMENTAL SETUP

The experimental test section, being one of the components in an experimental test facility, as shown in Figure 1, consisted of a tube-in-tube heat exchanger in a counterflow configuration. Distilled water was used as the working fluid for both streams, with the inner fluid being hot and the annulus fluid being cold. Thus, the inner fluid is being cooled, as is the case in chiller units. This differs from most other experimental setups where the fluid in the inner tube is heated at a constant heat flux (Allen and Eckert 1964; Ghajar and Tam 1991; Ghajar and Tam 1994; Petukhov et al. 1969).

Before entering the test section, the test fluid in the inner tube was heated to a temperature of 40°C–45°C (104°F–113°F) by means of a counterflow heat exchanger. The heating of the test fluid was made by means of a secondary flow loop containing water from a 1000 L (264 gal) reservoir. The temperature in this reservoir was maintained at approximately 60°C (140°F) by means of a 12 kW (41,000 Btu/h) electric heater.

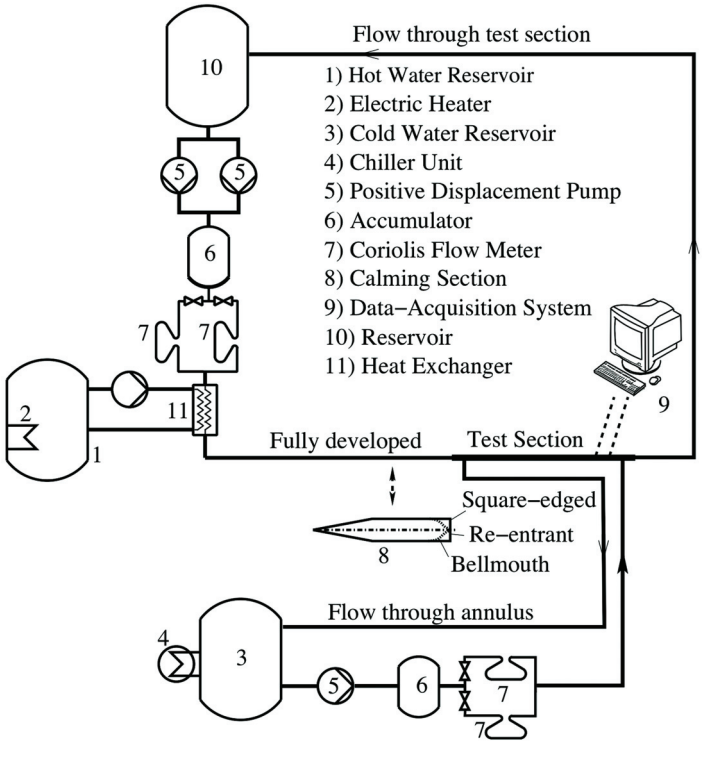

Figure 1. Schematic layout of the experimental system.

Fouling could also be a problem when using water as a working fluid. Therefore, filters were installed in the test loop to capture any dirt that might have formed. Further, the water was also changed on a regular basis to prevent the buildup of contamination. Heat transfer tests were performed after the experimental campaign, with results showing less than a 2% deviation of the data captured at the start of the campaign, showing that fouling of the tubes did not occur.

The test fluid was pumped through the system with two electronically controlled positive displacement pumps. The two pumps were installed parallel to one another and were used in accordance with the flow rate requirements. The pumps were of similar capacity, each having a maximum flow rate of 270 L/h (71 gal/h).

The cold water loop consisted of a 1000 L (264 gal) reservoir, which was connected to a chiller with a cooling capacity of 15 kW (51,000 Btu/h). The temperature inside the reservoir was maintained at 20°C (68°F) to prevent the risk of condensate forming on the test section if lower temperatures were used. The water was circulated through the system via an electronically controlled, positive displacement pump, which had a maximum flow rate of 2670 L/h (705 gal/h).

Implicit with the use of positive displacement pumps were flow pulsations, which were introduced into the system. This had an unfavorable effect on the stability of the flow, which was crucial when studying transitional flow. To decrease pulsations, a 70 L (18.5 gal) accumulator was installed before the flow meters and the test section. The accumulators were fitted with rubber bladders filled with air that dampened these fluctuations, resulting in a much more constant pressure at the inlet of the test section. A test was conducted to determine the effect of the accumulators on the flow rate. It was found that without them, the mass flow rate fluctuations varied between 0.3% and 0.6%, while with the accumulators, the flow fluctuations never varied more than 0.05%. This, in combination with the low flow rate pumps, enabled Reynolds numbers as low as 100 to be achieved.

From the accumulators, the water flowed through a set of Coriolis flow meters, which measured the mass flow rate. A total of four flow meters of different capacities were used (two that were parallel on the fluid-side) according to the flow rate requirements. After the flow meters, the fluids flowed through the experimental test section and then back into the reservoirs.

Flow rates were controlled by means of frequency drives, which were connected to the positive displacement pumps. In turn, the frequency drives were connected to a personal computer via a data-acquisition system from which the frequencies could be set. The computer would give a voltage output, which the drives converted to a representative frequency. The finest voltage increments were in the order of 0.02 V, which in terms of Reynolds number were in the order of $\Delta \mathrm{Re} = 20$.

Prior to the flow entering the test section, the flow first went through a calming section. The purpose of the calming section was two-fold: first, to remove any unsteadiness in the flow and to ensure a uniform velocity distribution, and second, to house the different types of inlets to be investigated. Figure 2 gives a schematic view of the calming section. The calming section was based on work conducted by Ghajar and Tam (1994) and was made from clear acrylic. Bleed valves were installed at the top of this section at several axial positions, ensuring that all of the air that was trapped could be removed. Sight glasses were also installed after the test section to see if any air bubbles were present. The calming section also consisted of a 5° diffuser, which increased from a diameter of 15 mm (0.59 in.) to 140 mm (5.5 in.). This angle was chosen such to prevent flow separation from the diffuser wall. Three screens were located 70 mm after the diffuser and were separated 105 mm (4.1 in.) apart. These screens had an open-area ratio (OAR) of 0.31 (60 holes each with a diameter of 10 mm [0.39 in.]). The OAR is the ratio of the area occupied by the holes to the total area occupied by the whole screen. A honeycomb section was located 155 mm (6.1 in.) downstream of the screens, which had an OAR of 0.92 and a length of 100 mm (3.94 in.). Prior to and after the honeycomb, was a wire mesh, with the wires having a

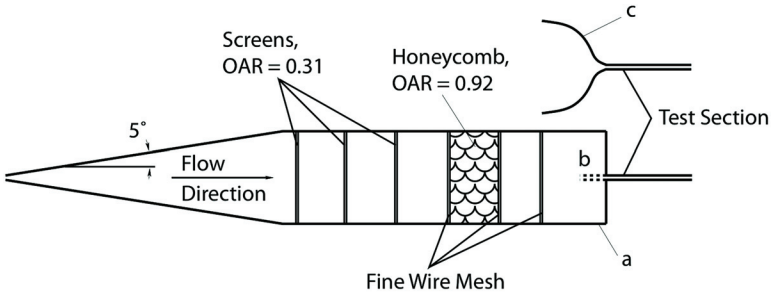

Figure 2. Schematic view of the calming section with three different inlet configurations that could be housed, namely (a) square-edged, (b) re-entrant, and (c) bellmouth. OAR is the open-area ratio.

diameter of 0.8 mm (0.03 in.) and the OAR being 0.54. Another fine wire mesh was inserted prior to the inlet nozzles situated 170 mm (6.7 in.) downstream from the honeycomb. This mesh had a wire diameter of 0.3 mm (0.012 in.) and an OAR of 0.17.

Three different inlets could be housed on the calming section, namely a square-edged, re-entrant, and a bellmouth inlet. These inlets are also shown in Figure 2 as items a, b, and c, respectively. The calming section was designed such that the inlets could easily be interchanged. The square-edged inlet is characterized by a sudden contraction of the flow (from 140 mm [5.5 in.] to 14.8 mm [0.58 in.] or 17.7 mm [0.70 in.], depending on the tube being tested). This is a typical situation encountered in the header of a shell-and-tube exchanger. The re-entrant inlet makes use of the square-edged inlet, except that the tube slides into the inlet by a one-tube diameter. This would simulate a floating header in a shell-and-tube heat exchanger. The third type of inlet is the bellmouth. The bellmouth is characterized by a smooth contraction (a contraction ratio of 8.8). The shape of the bellmouth was calculated with the method suggested by Morel (1975). The use of a bellmouth is thought to help in the reduction of fouling, although practical application is uncommon in heat exchangers. With the use of different inlet geometries, the velocity profile in the test section is always developing. Therefore, a fourth type of inlet was used to obtain a fully developed velocity profile. This was done by using the bellmouth inlet in combination with an extra length of tubing that had the same diameter as the test section. The length of the tubing was determined by Durst et al. (2005), which required a minimum length of 120-tube diameters. To ensure this minimum was met, the length of the inlet was chosen as 160-tube diameters. Throughout the paper this inlet will be referred to as the *fully developed inlet*. A schematic of the inlets relative to the test section is shown in Figure 3.

The test section consisted of a counterflow tube-in-tube heat exchanger. All the test sections were manufactured from hard-drawn copper tubes, which were insulated with 25 mm (0.98 in.) of thick insulation with a thermal conductivity of 0.034 W/m·K (0.0196 Btu/h·°F). The maximum estimated relative heat losses to the environment, based on a simple one-dimensional heat transfer calculation, were less than 1% of the total heat transfer in the test section and were to be obtained at the lower end of the Reynolds numbers considered. The total length of each test section was approximately 5 m (16.4 ft). The two tubes tested had a nominal outside diameter of 15.88 mm (5/8 in.) and 19.02 mm (3/4 in.), each having an inner diameter of 14.482 mm (0.57 in.) and 17.6 mm (0.69 in.), respectively.

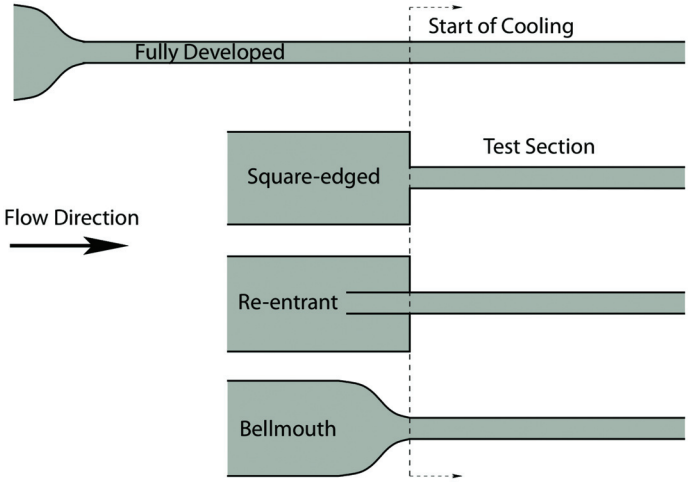

Figure 3. Illustration of the different inlet geometries relative to the test section.

The annulus outer diameters were chosen such that the space between the annulus and the inner tube was small, ensuring high flow velocities. So, turbulent flow was present within the annulus, which ensured that the annulus had a small thermal resistance compared with the inner tube. A 20.7 mm (0.81 in.) inside diameter annulus was used for the 15.88 mm (5/8 in.) diameter tube, and a 26.3 mm (1 in.) inside diameter annulus was used for the 19.02 mm (3/4 in.) tube. The respective hydraulic diameters were 4.81 mm (0.19 in.) and 7.21 mm (0.28 in.). To prevent sagging and the outer tube touching the inner tube, capillary tube was wound around the outer surface of the inner tube at a constant pitch of approximately 60°. This also further promoted mixing inside the annulus.

The high flow rate that could be obtained for the cold water loop, which flowed through the annulus, not only ensured that the thermal resistance of the annulus was much smaller than that of the inner tube, but it also ensured that the variation in the inner tube wall temperature from inlet to outlet was kept at a minimum. The wall temperature never varied more than 3°C (37.4°F) along the 5 m (16.4 ft) length tube for high-laminar Reynolds number flows. Laminar data are normally represented in terms of the boundary condition either being uniform heat flux or constant wall temperature. The difference in heat transfer values between the two boundaries in pure laminar flow (no secondary effects) is approximately 20%. However, for the present study, although slightly varying, the wall temperatures were much closer to the constant wall temperature boundary than the uniform heat flux boundary, and all comparisons were made to such.

Heat transfer rates varied between 1000 W (3400 Btu/h) and 15,000 W (51,000 Btu/h) and was dependent on the inner tube flow rate. This translated to a heat flux variation of 4 kW/m^2 (1286 Btu/h) to 61 kW/m^2 (19,350 Btu/h) from low to high inner tube Reynolds numbers.

A schematic layout of the test section is given in Figure 4. T-type thermocouples with a nominal wire diameter of 0.2 mm (0.007 in.) and a limit of precision of 0.1°C (0.18°F) were used. A total of 53 thermocouples were used, with 12 of them assigned to measure the inner tube and annulus inlet and outlet temperatures. Thirty-six thermocouples were placed around the periphery of the inner tube's outer wall at nine axial stations, while the remaining five were placed on the annulus outer wall. Small grooves on the outside of the inner

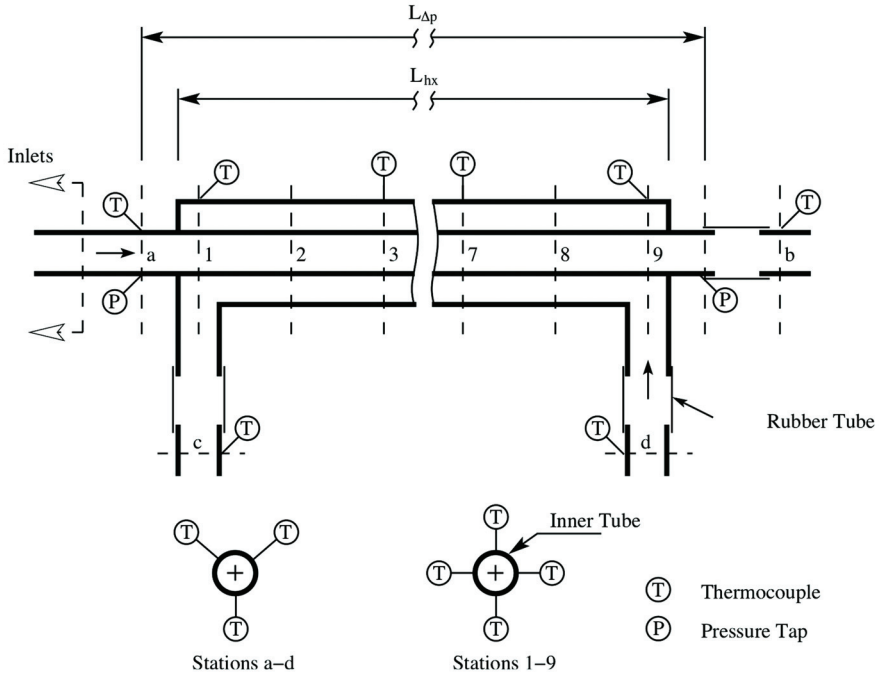

Figure 4. Schematic layout of the test section.

tube were made to place the wall thermocouples. The thermocouples were then soldered into these grooves, which ensured that not only good electrical contact was made, but also that they were flush with the wall. The average temperature measurements on the outer wall of the annulus, together with the inlet and outlet temperature measurements, were used to more accurately estimate the bulk temperature of the water in the annulus (unlike using the average of the inlet and outlet temperature only). All the thermocouples were calibrated with a Pt-100 temperature probe, which itself was calibrated to within 0.01°C (0.018°F).

Differential pressure measurements were made possible by means of two pressure taps inserted at the inlet and outlet of the inner tube. To ensure the pressure taps did not influence the pressure readings, their diameters were kept below 10% of the inner diameter of the tested tube (Rayle 1959), while great care was taken to remove the burrs formed by the drilling process. The pressure transducers were calibrated with a water manometer that had an uncertainty of 0.17%.

Temperatures and pressures were captured by a data-acquisition system. Each data point consisted of 100 samples taken over a period of 2 min. Therefore, data was captured at a rate of approximately 1.2 Hz. These samples were then averaged to represent one data point. In developing the correlations, however, all the data, not the averaged data, was used.

A full experimental uncertainty analysis was performed on the system by the method suggested by Kline and McClintock (1953). Uncertainties for the operating conditions are given in Table 1. The uncertainties listed not only include the values due to the propagation of error, but also the random errors from the measurements. The full uncertainty analysis can be found in Olivier (2009).

Table 1. Experimental Range and Uncertainties

	Value	Uncertainty
$\dot{m}_i$	0.0087–0.0822 kg/s (0.019–0.18 lb/s)	0.664%–0.412%
$\dot{m}_o$	0.429–0.445 kg/s (0.95–0.98 lb/s)	0.164%–0.260%
T_{iin}, T_{iout}, T_{oin}, T_{oout}	20.35°C–65.67°C (68.63°F–150.2°F)	0.011°C–0.46°C (0.02°F–0.83°F)
T_o	20.9°C–23.67°C (69.62°F–74.61°F)	0.014°C–0.032°C (0.025°F–0.058°F)
T_{wo}	21.33°C–25.53°C (70.39°F–77.95°F)	0.011°C–0.055°C (0.02°F–0.099°F)
T_{wi}	21.34°C–25.61°C (70.41°F–78.1°F)	0.011°C–0.055°C (0.02°F–0.099°F)
T_i	32.98°C–41.97°C (91.36°F–107.55°F)	0.176°C–0.857°C (0.317°F–0.543°F)
T_{lmtd}	12.16°C–18.18°C (53.89°F–64.72°F)	0.172°C– 0.855°C (0.310°F– 0.539°F)
$\dot{Q}_i$	1598–10,954 W (5453–37,376 Btu/h)	0.71%–0.49%
UA	131.5–605.8 K/W (69.32–319.36 °F·h/Btu)	1.02%–1.08%
Re	1026–11,485	1.20%–1.08%
Nu	13.06–62.20	1.44%–1.58%
Pr	4.17–5.06	±1.42%
Δp	45–1583 (0.0065–0.2296 $lb_f/in.^2$)	4.71%–1.59%
α_i	558–2710 W/m·K (98.27–477.58 Btu/h·ft^2·°F)	1.04%–1.22%
f	0.0085–0.0212	2.84%–11.28%

DATA REDUCTION

The inner tube's average heat transfer coefficient was obtained by making use of the overall heat transfer coefficient and the sum of the resistances, given by

$$\alpha_i = \frac{1}{A_i}\left[\frac{1}{UA} - R_w - \frac{1}{\alpha_o A_o}\right]^{-1}. \quad (1)$$

UA is the overall heat transfer coefficient, which can be obtained by means of the overall heat transferred and the log-mean temperature difference, calculated from the inlet and outlet temperatures of the inner tube and annulus as follows:

$$UA = \frac{\dot{Q}_i}{T_{lmtd}} \tag{2}$$

$\dot{Q}_i$ is the heat transferred in the inner tube, calculated as

$$\dot{Q}_i = \dot{m}_i \Delta h_i , \tag{3}$$

where $\dot{m}_i$ and Δh_i are, respectively, the inner-tube mass flow rate and the enthalpy difference between the inlet and outlet of the inner tube. The enthalpies were obtained from IAPWS (2003), which were based on the fluid temperature. The annulus heat transfer coefficient was calculated by means of the annulus bulk temperature and the average inner-tube, outer-wall temperature measurements. The bulk and average wall temperatures were obtained by numerically integrating the local temperatures along the length of the tube by making use of the trapezium rule. Therefore, only a single bulk value for the annulus heat transfer coefficient was obtained. This is given by the following equation:

$$\alpha_o = \frac{\dot{Q}_i}{A_o(T_o - T_{wo})} \tag{4}$$

The inner-tube heat transfer rate was used for all the calculations, since it had the lowest uncertainty. Throughout the tests, the annulus flow rate was kept as high as possible, as this reduced the thermal resistance of the annulus, reducing its influence in Equation 1, and hence decreasing the equation's overall uncertainty. On average, the annulus thermal resistance was only 6% the value of the inner tube. All fluid properties were obtained from Wagner and Pruß (2002). Experimental data were only captured once an energy balance of less than 1% was achieved. At low inner-tube Reynolds numbers (<6000), this requirement was not met due to the high annulus flow rate and its uncertainty. Tests were, however, conducted as checks by substantially lowering the annulus flow rate. These tests proved that the heat transfer error in the inner tube at low Reynolds numbers was indeed less than 1%.

The Darcy-Weisbach friction factors were determined using the following equation:

$$f = \frac{2\Delta p D_i}{\rho u^2 L_{\Delta p}} \tag{5}$$

The bulk fluid properties used for the calculation of the Reynolds, Prandtl numbers, etc., were calculated at the average inner-tube fluid temperature, which, in turn, was determined by the resulting heat transfer coefficient, Equation 1, as

$$T_i = \frac{\dot{Q}_i}{\alpha_i} + T_{wi} . \tag{6}$$

Heat transfer results were expressed in terms of the Colburn *j*-factor, defined as

$$j = \frac{\mathrm{Nu}}{\mathrm{RePr}^{1/3}} . \tag{7}$$

RESULTS

Adiabatic Friction Factors

Figure 5 gives the adiabatic friction factor results for the 15.88 mm (5/8 in.) and 19.02 mm (3/4 in.) smooth tubes with a fully developed inlet. A total of 404 data points (298 for the 15.88 mm [5/8 in.] tube and 106 for the 19.02 mm [3/4 in.] tube) were used. Each run consisted of data being captured in increments of increasing, as well as decreasing, Reynolds numbers. This was done to investigate any hysteresis in the transition region. Included in the graph is the Blasius correlation ($f = 0.316\ \mathrm{Re}^{-0.25}$) for turbulent flow, as well as the Poiseuille relation ($f = 64/\mathrm{Re}$) for fully developed, isothermal laminar flow (ASHRAE 2009). Also included are the data from Senecal and Rothfus (1953), Nunner (1956), Koch (1960), Patel and Head (1969), Ghajar and Madon (1992), García et al. (2005), and Churchill's (1977) correlation.

The laminar and turbulent results were in excellent agreement with the theoretical models, with the Poiseuille relation predicting the data to within 1.5% with a maximum root mean square deviation of less than 4.5%. The turbulent results were predicted by the Blasius equation on average to within 0.7%, with a maximum deviation of less than 2.5%.

Transition from laminar to turbulent flow started at a Reynolds number of approximately 2100 and ended at approximately 2900. These were typically the values quoted in most fluid dynamics textbooks. Differences between the data for increasing and decreasing Reynolds numbers were less than 0.7%, with a maximum deviation of 4.3%. Hysteresis in the transition regime was negligible. Further, the current experimental data and the work of others are in excellent agreement. The work of Ghajar and Madon (1992), who used a similar setup with a

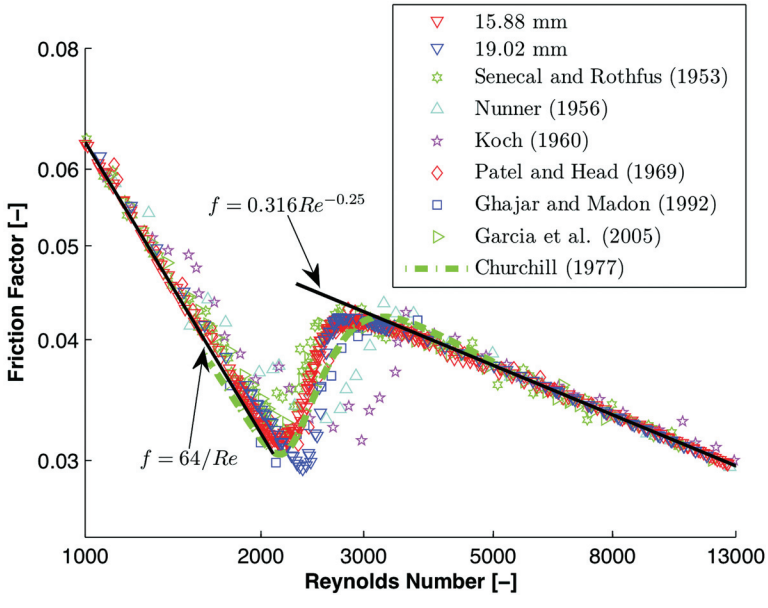

Figure 5. Adiabatic friction factors for the 15.88 mm (5/8 in.) and 19.02 mm (3/4 in.) smooth tubes with a fully developed inlet.

bellmouth inlet with measurements in the fully developed region, also shows excellent agreement with the current data. This also validates the accuracy of the pressure drop measurements.

Figure 6 shows the adiabatic friction factor results for the two diameters of smooth tubes with various inlet profiles. This figure consists of a total of 1478 data points. Also included are the fully developed friction factors of Tam and Ghajar (1997). At this point, a distinction between the data sets should be made. Tam and Ghajar's (1997) data are for fully developed flow, as these measurements were taken far downstream from the inlet. The current experimental data are for developing flow, which might include fully developed flow, as measurements were made across the complete 5 m (16.4 ft) length of the tube. Similarities between the data sets are clear, though. Transition for the square-edged inlet is delayed more than for the re-entrant inlet, while the bellmouth inlet delays transition the most.

In general, though, transition from laminar to turbulent flow commences at different Reynolds numbers. For the re-entrant inlet, transition appeared to differ very little from the fully developed value, while the square-edged and bellmouth inlets delayed transition quite considerably. This is also confirmed in Figure 7, which shows the relative friction factor standard deviation as a function of the Reynolds number for each tube and inlet. The difference between the 15.88 mm (5/8 in.) and 19.02 mm (3/4 in.) tubes for the first two inlets is negligible. However, for the bellmouth inlets, there is a definite difference between the two, with the 19.02 mm (3/4 in.) tube showing transition to start at a Reynolds number of approximately 12,000. Transition for the 15.88 mm (5/8 in.) tube

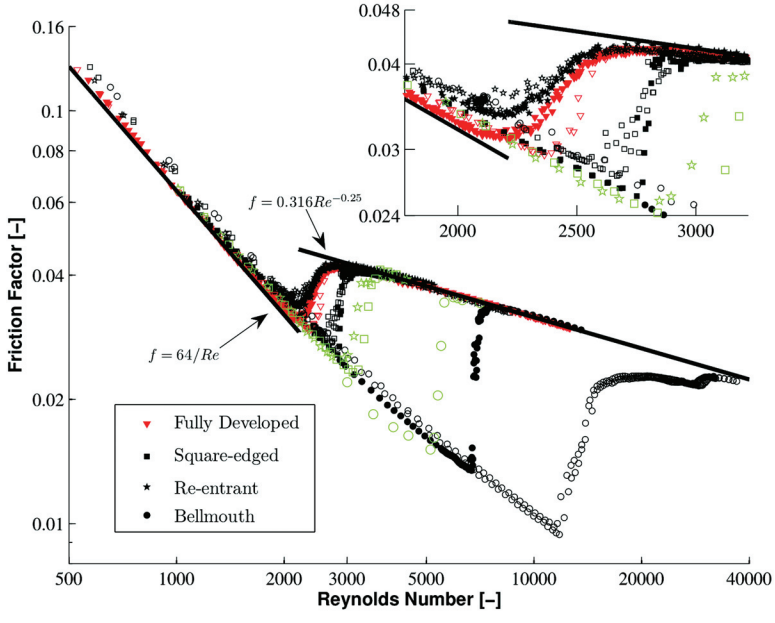

Figure 6. Adiabatic friction factors for the 15.88 mm (5/8 in.) and 19.02 (3/4 in.) smooth tubes with various inlets (solid markers are for the 15.88 mm [5/8 in.] tubes, while the empty ones are for the 19.02 mm [3/4 in.] tubes). Green markers represent Tam and Ghajar's (1997) data. The inset is to enlarge the results between Reynolds numbers of 2000 and 3000.

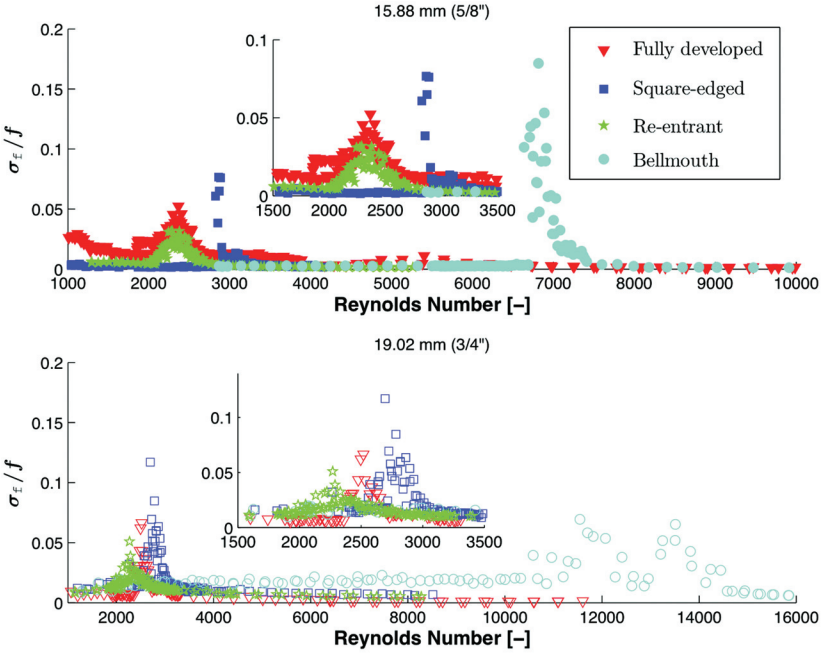

Figure 7. Friction factor fluctuations, showing the start and end of transition for the different inlets.

starts at approximately 7000. As this difference was unexpected, the measurements were repeated for both tubes, although the same results were obtained. This difference in transition for the different inlets, as noted by Ghajar and co-workers, is due to the amount of turbulence the different inlets generate, with the re-entrant generating the most.

The difference between the 15.88 mm (5/8 in.) and 19.02 mm (3/4 in.) bellmouth entrances can be explained by the fact that the physical bellmouth entrances used for the two tubes were different, as each had a different contraction ratio, and they were manufactured at different dates during the project. This could mean that their internal roughness might have been different due to the manufacturing technique, which might have differed. This difference in roughness will have an effect on the transition, as noted by Tam and Ghajar (1998), showing that the use of different mesh sizes prior to the inlet has an effect on transition, with the finer mesh delaying transition the most (this would also explain why transition for the 19.02 mm [3/4 in.] tube for fully developed flow is delayed slightly more than transition for the 15.88 mm [5/8 in.] tube). Since the current experiments used the same mesh for both diameter tubes, the only difference would be the bellmouth roughness. The difference in the contraction ratio could also have played a role, but there was not enough evidence to support this. The fact is, though, that transition was greatly influenced by the type of inlet used, with transition being the earliest for the inlet generating the most turbulence, or having the most severe inlet geometry.

Laminar flow results for the various inlets, unlike the fully developed results, were slightly higher than the laminar friction factor obtained from the Poiseuille relation. The main reason for this was the growing hydrodynamic boundary layer from the inlet of the tube. Due to the flow

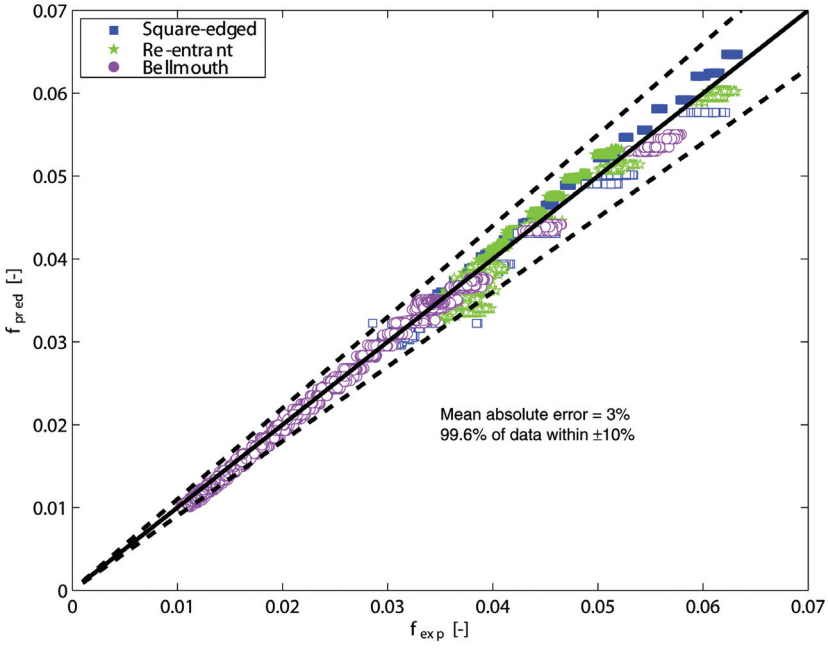

Figure 8. Developing flow laminar friction factor results compared with Shah's correlation (1978).

being in a closure (the tube), the boundary layer grew on all sides simultaneously. However, due to continuity requirements, a retardation near the tube wall caused the core at the center of the flow to speed up, which suppressed the boundary layer, causing it to become fully developed at distances much further than those predicted by the flat-plate theory (White 1991). This suppression of the boundary layer and the acceleration of the center core caused an increase in shear, and hence, an increase in friction. Figure 8 shows a comparison of the laminar friction factors for the developing flow inlets against Shah's (1978) correlation. There is excellent agreement between the data and the correlation, with the data being predicted with a mean absolute error of 3%, with 99.6% of the data being predicted to within 10%. Ghajar and Madon (1992) obtained similar results, however, only the bellmouth inlet showed good agreement for Reynolds numbers less than 1500 with this correlation.

Heat Transfer

The heat transfer results for the smooth tubes with all the inlets are shown in Figure 9 in terms of the Colburn *j*-factor. This figure consists of a total of 581 data points. For the 15.88 mm (5/8 in.) smooth tube, the number of data points is 83 (fully developed), 59 (square-edged), 27 (re-entrant), and 72 (bellmouth). For the 19.02 mm (3/4 in.) tube, the data points are 45 (fully developed), 57 (square-edged), 101 (re-entrant), and 137 (bellmouth). Also included in the graph are 811 data points (green) from the same experimental facility for the 15.88 mm (5/8 in.) tube for the four inlets using a 50% v/v water-propylene glycol mixture. Further, Ghajar and Tam's (1994) data (in red) are included. It should be

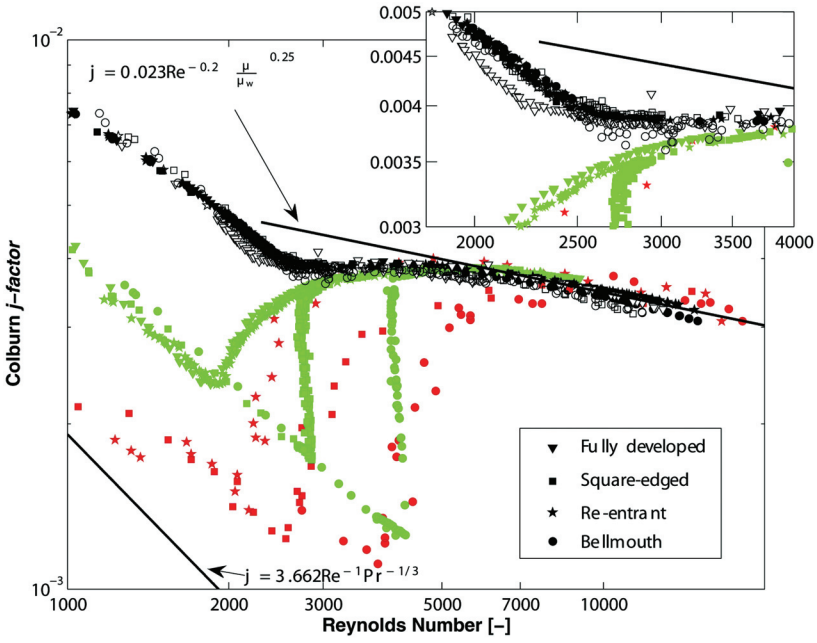

Figure 9. Smooth tube heat transfer results in terms of the Colburn *j*-factor for all of the inlets. Solid markers represent the 15.88 mm (5/8 in.) tube, and empty markers represent the 19.02 mm (3/4 in.) tube (black = water, green = water-propylene glycol for the 15.88 mm [5/8 in.] tube, red = data from Ghajar and Tam [1994]).

noted that Ghajar and Tam's (1994) data is for fully developed flow, while the current data is for developing flow. The water-propylene glycol data were only added for comparison reasons. The figure shows that water has some special characteristics regarding laminar flow and transition.

Turbulent results for all the data show excellent agreement with Colburn's correlation (1933) as modified by Sieder and Tate (1936), which included the viscosity correction ratio. In terms of the Colburn *j*-factor, this is given by

$$j = 0.023\ \mathrm{Re}^{-0.2}\left(\frac{\mu}{\mu^{w}}\right)^{0.25}. \tag{8}$$

Figure 10 shows the comparison of the turbulent heat transfer data taken for $\mathrm{Re} > 4000$ with the Sieder and Tate (1936) correlation and the Gnielinski (1976) correlation, modified to incorporate entrance effects, which is given as

$$\mathrm{Nu} = \frac{(f/8)(\mathrm{Re}-1000)\mathrm{Pr}}{1+12.7\sqrt{(f/8)}(\mathrm{Pr}^{2/3}-1)}\left[1+\left(\frac{D_i}{L}\right)^{2/3}\right]\left(\frac{\mu}{\mu_w}\right)^{0.25}, \tag{9}$$

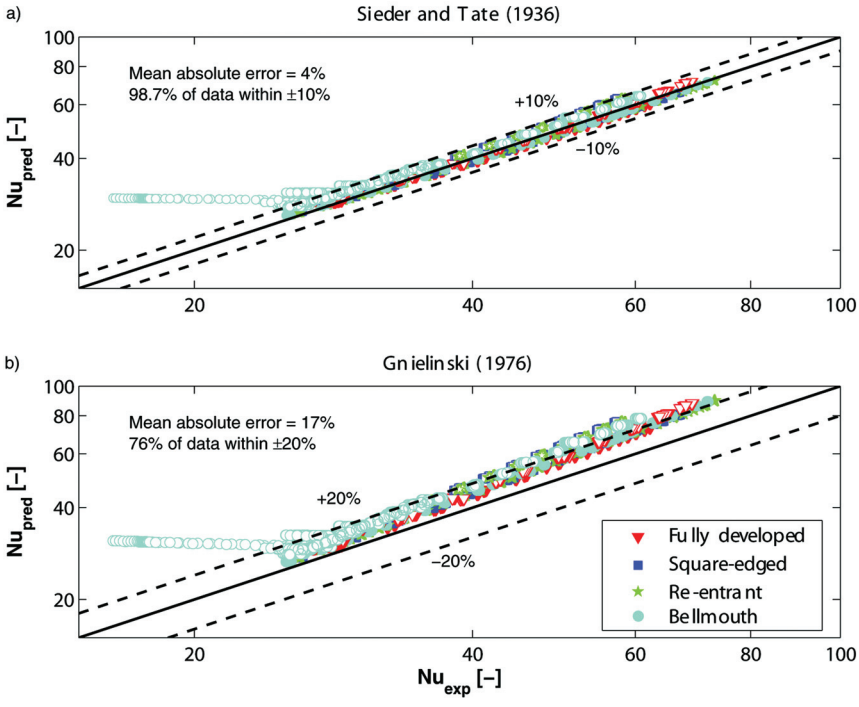

Figure 10. Comparison of turbulent results ($Re > 4000$) for the fully developed and developing flows against the (a) Sieder and Tate (1936) and (b) Gnielinski (1976) correlations.

where the friction factor of Filonenko (Lienhard and Lienhard 2003) is used, which is also adjusted by making use of the viscosity ratio, as given by

$$f = (1.82 \ln \mathrm{Re} - 1.64)^{-2}\left(\frac{\mu}{\mu_w}\right)^{-0.24}. \quad (10)$$

Sieder and Tate's (1936) correlation predicted the data with a mean absolute deviation of 4%, predicting 99% of the data to within 10%. Gnielinski's (1976) correlation, predicted the data with a mean absolute error of 17%, predicting 76% of the data to be within 20%, and 98% of the data to within 30%. Note that at the lower Nusselt numbers there was a large deviation in the data. This data was from the bellmouth entrance for the 19.02 mm (3/4 in.) tube, which had a slight delay transition.

Laminar flow results were much higher than predicted by the theoretical constant of 3.66 or 4.36 (ASHRAE 2009) for the constant wall temperature or uniform heat flux boundary condition. (The Reynolds numbers in the annulus were kept very high relative to the inner tube, resulting in wall temperatures that varied little along the length of the tube). The higher heat transfer results were attributed to the buoyancy-induced secondary flow in the tube due to the difference in density at the center and the wall of the tube. The Oliver (1962) and Shome and Jensen (1995) correlations, designed to incorporate these natural convection effects for constant wall temperature boundaries, predicted 95.7% and 99.8% of the laminar data from a Reynolds number of 1000 to 2100 to within 10%, respectively, with a mean absolute error of 6% and 3%,

respectively. This is shown in Figure 11. Figure 12 shows the flow regime map developed by Metais and Eckert (1964). This specifically shows that most of the laminar data fall within the mixed convection regime, further validating the effect of secondary flows.

The water-propylene glycol data and Ghajar and Tam's (1994) data in Figure 9 compare fairly well with each other with regard to transition, although laminar results for the mixture are somewhat higher. The difference between the mixture and Ghajar and Tam's (1994) data could be due to the fluid Prandtl numbers differing. The data for the mixture had an average Prandtl number of about 26, while Ghajar and Tam's data was between 40 and 160 in the laminar region. The Prandtl number for the water results were in the order of 5 to 6, with the laminar results being the highest. This shows that the Prandtl number might actually have a negative effect on mixed convection and secondary flows. This is supported by Siegwarth et al. (1969) who performed a numerical analysis of the flow field. They showed that for Pr = 1 and a large Rayleigh number the diffusion terms are small in comparison with the convective terms, while for large Pr, the convective terms are small in comparison with the diffusion terms. This implies that for large Prandtl number fluids the primary flow is independent of the secondary flow.

For the water-propylene glycol data (green markers in Figure 9), for the square-edged and bellmouth inlets, the transition lines had a negative gradient. The reason for this is that even though the mass flow rate increased, due to the increase in mixing in this region, the viscosities obtained from the bulk fluid properties increased, causing a decrease in the Reynolds numbers.

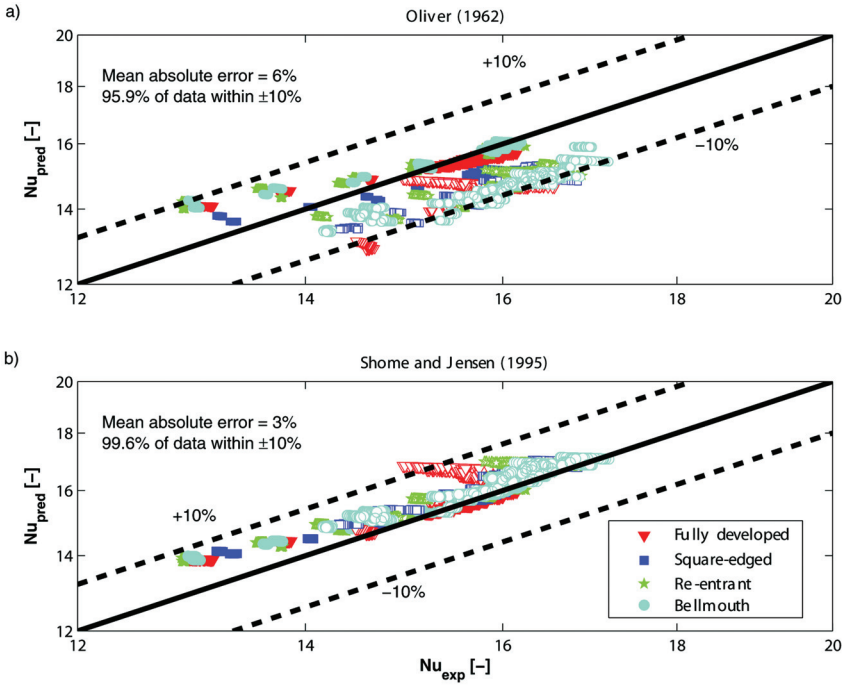

Figure 11. Laminar Nusselt numbers compared with Oliver's (1962) and Shome and Jensen's (1995) correlations. Solid markers denote the 15.88 mm (5/8 in.) tube, and the empty markers denote the 19.02 mm (3/4 in.) tube.

All of the results for the water data for different types of inlets show a smooth transition from laminar to turbulent flow. These results are similar to those of Manglik and Bergles (1993a), who used twisted tape inserts. The inserts caused a swirl in the flow, with the result being that there was a competing effect between the swirl motion and turbulent flow. For the current data, the swirl motion can be replaced by the secondary flows due to natural convection, which also compete with the turbulent flow.

Transition for water, however, is independent of the type of inlet used. The results gathered by Ghajar's laboratory showed that transition was greatly influenced by inlet disturbance. The effect of heat transfer, which induces secondary flows, actually dampens the effect of the turbulence generated at the inlet, thus almost nullifying its presence. These results are confirmed in Figure 13, which shows the relative heat transfer standard deviation (in terms of the Colburn *j*-factor) as a function of the Reynolds number. Note that there is a deviation for the bellmouth inlet for the 19.02 mm (3/4 in.) tube. This shows that this inlet still has an influence on transition, but it is much less than what was found for the adiabatic case (Figure 6). This also explains the deviation found in the comparison of the turbulent correlations in Figure 10. Mori et al. (1966) also postulated that inlet disturbance could be negligible for high enough Rayleigh numbers. Nagendra (1973) made a similar postulation, stating that for high enough values of the product of Reynolds and Rayleigh numbers and diameter-to-length ratios, inlet disturbances could have no effect on transition. From Nagendra's graphs, the value of this product is around 10^6. For the current experimental data, this product had a value of between

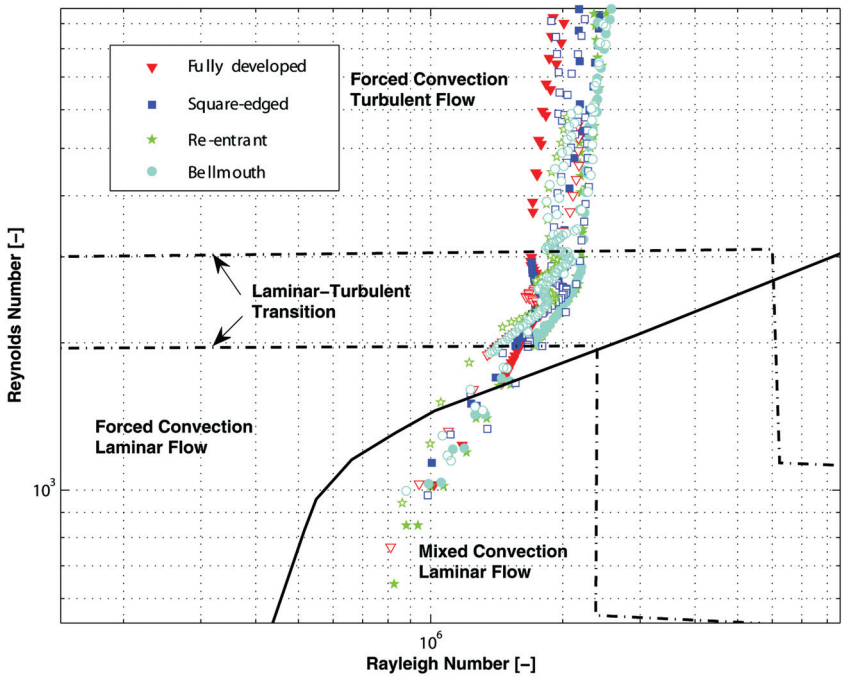

Figure 12. Flow regime map of Metais and Eckert (1964) for the smooth tubes with different inlets. Solid markers represent the 15.88 mm (5/8 in.) tube, while the empty markers represent the 19.02 mm (3/4 in.) tube.

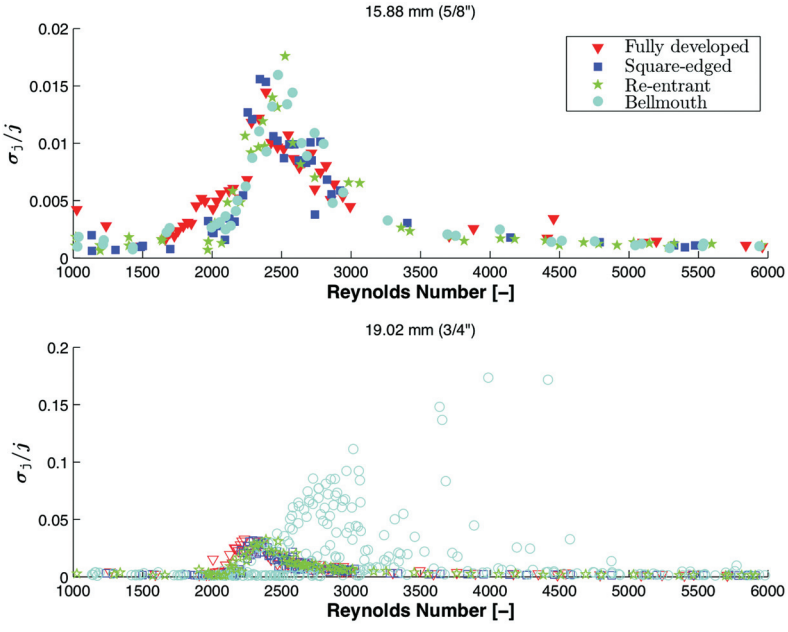

Figure 13. Heat transfer fluctuations as a function of the Reynolds number for fully developed and developing flow.

3×10^6 and 3×10^7. From the results, it was found that transition for water occurred at the same Reynolds numbers, starting and ending at 2100 and 3000, respectively. These results were confirmed by pressure drop data, which were measured totally independent of the heat transfer data, showing exactly the same trends.

DIABATIC PRESSURE DROP

Figure 14 shows the diabatic friction factors as a function of the Reynolds number. Included in the graph are the Poiseuille relation for laminar flow, the Blasius correlation for adiabatic flow, and the recommended Filonenko correlation with the variable fluid property correction as suggested by Lienhard and Lienhard (2003). What is noticeable is the overall increase in friction factors when compared with the adiabatic predictions. Turbulent results correlated fairly well with the viscosity correction, predicting 99.7% of the data to within 10% with a mean absolute error of 2.4%. For the laminar region, friction factors were on average 35% higher than predicted by the Poiseuille relation. Even with a viscosity correction, the prediction only improved by 4%. This increase in friction factor can be attributed to the secondary flow effects, with data from Nunner (1956) showing similar results. Tam and Ghajar (1997) also attributed the increased fully developed friction factors they obtained to secondary flow. They further found that by increasing the overall heat flux, the laminar friction factors increased. Although heat fluxes for the current setup could not be varied for a fixed Reynolds number, it is seen that the friction factors approach the Poiseuille relation as the Reynolds numbers decrease, which in turn also results in a decrease in heat flux. This implies that since the friction factor is proportional to the wall shear stress, which, in turn, is proportional to the velocity gradient at the wall, secondary flow distorts the velocity profile in such a way that the

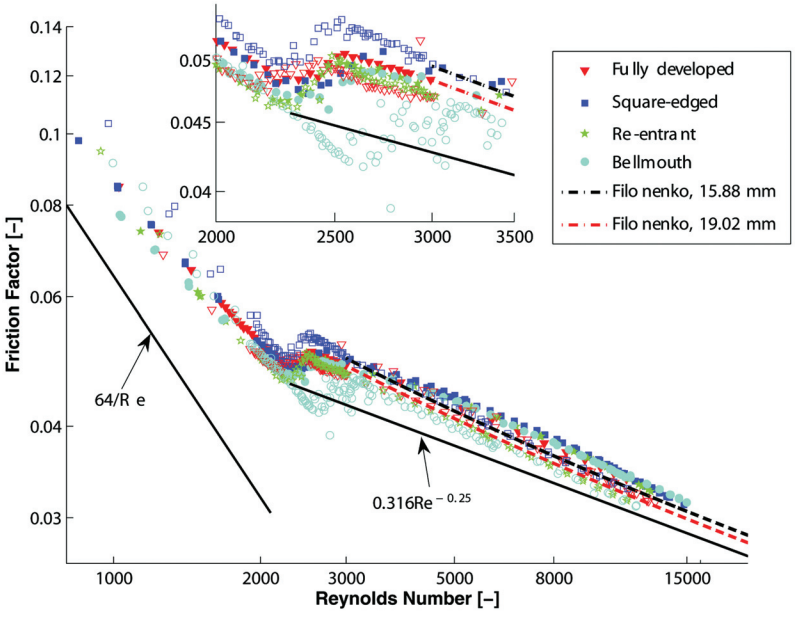

Figure 14. Diabatic friction factors for smooth tubes with different inlets. Solid markers are 15.88 mm (5/8 in.) data, while empty markers are 19.02 mm (3/4 in.).

gradient near the wall is much steeper. This would then give rise to the higher friction factors. Many numerical and experimental studies have been performed showing this distortion (Faris and Viskanta 1969; Ou and Cheng 1977; Hwang and Tsai 1997; Maré et al. 2006). Mikesell (1963) suggested and observed that in certain extreme cases backflow might even occur.

Looking at the transition from laminar to turbulent flow, it can be observed that the s-curve for the diabatic case was much smaller than that witnessed for the adiabatic case. This also confirms the heat transfer results with regard to transition being less severe in the sense that there was no sudden (or very little) increase in friction factor values in this region. This effect is analogous to twisted tape inserts, as discussed by Manglik and Bergles (1993b), where the swirl induced by the tapes not only increases the friction factors, but also causes a smooth transition to turbulence. This is due to the secondary flow (swirl flow) having a competing effect on the onset of turbulence. Transition also occurred at the same Reynolds number, which is also confirmed by a plot of the relative diabatic friction factor fluctuations, as shown in Figure 15. Only the data for the 19.02 mm (3/4 in.) tube are shown, as the 15.88 mm (5/8 in.) data for this part was corrupted. However, the results would look similar. Note that once again the bellmouth inlet showed a slight delay in transition, exactly the same as was shown in the heat transfer fluctuations (Figure 13). What is important to notice is that the same results regarding the start and end of transition were obtained by two totally independent measuring methods.

CORRELATION

Prior to developing a correlation, a comparison will be made to the correlations developed by Tam and Ghajar (2006) for heat transfer for the different inlets. This comparison for all the inlets is shown in Figure 16. The figure shows that transition is predicted rather poorly. This,

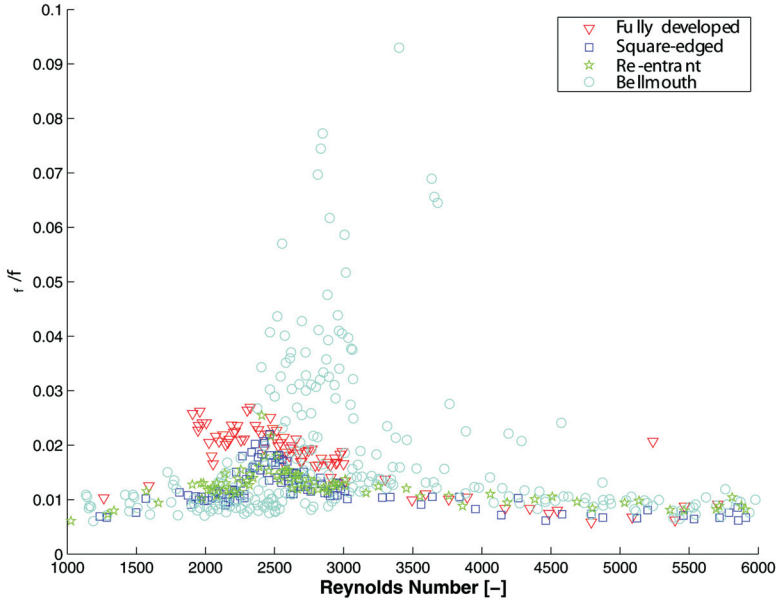

Figure 15. Diabatic friction factor fluctuations for fully developed flow for the 19.02 mm (3/4 in.) tube.

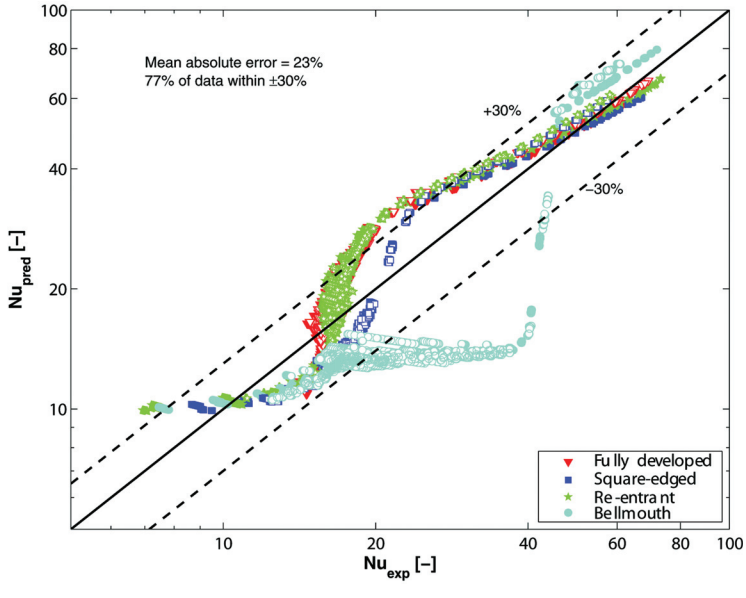

Figure 16. Heat transfer data compared with Tam and Ghajar's (2006) correlation.

however, is not due to the correlation, but rather the difference in fluids. Tam and Ghajar's (2006) correlation was developed for a fluid with a Prandtl number ranging from 40 to 160 for the laminar and transition regions. Further, it was developed for a fluid being heated with a wall-to-bulk viscosity ratio ranging from 1.2 to 3.8 for the same regions. The Prandtl number and viscosity ratio for the current experimental data ranged from 4 to 5 and 0.69 to 0.77, respectively. Further, as was shown from the heat transfer results and the discussion, transition was independent of the inlet disturbance for the low Prandtl number fluid, while the correlation was clearly inlet-dependent. However, there was good agreement for the higher Nusselt number values, where the flow was turbulent. This is understandable since Tam and Ghajar's (2006) correlation in this region is a variant of the Sieder and Tate (1936) correlation, which was in excellent agreement with the experimental data.

The diabatic laminar friction factors were compared to Tam and Ghajar's (1997) diabatic friction factor correlation, which is given as

$$f = \frac{64}{\mathrm{Re}}\left(\frac{\mu}{\mu_w}\right)^m,\ m = 1.65 - 0.013\mathrm{Pr}^{0.84}\mathrm{Gr}^{0.17}. \tag{11}$$

Figure 17a shows the experimental data against the prediction of Equation 11. As can be seen, there is a very poor prediction. However, since this correlation was developed for the heating of the fluid, the viscosity ratio is greater than 1. By changing the power of the viscosity ratio to $-m$, the comparison is much better, as is evidenced in Figure 17b. The correlation predicts almost 80% of the data to within 20%, with a mean absolute error of 15%.

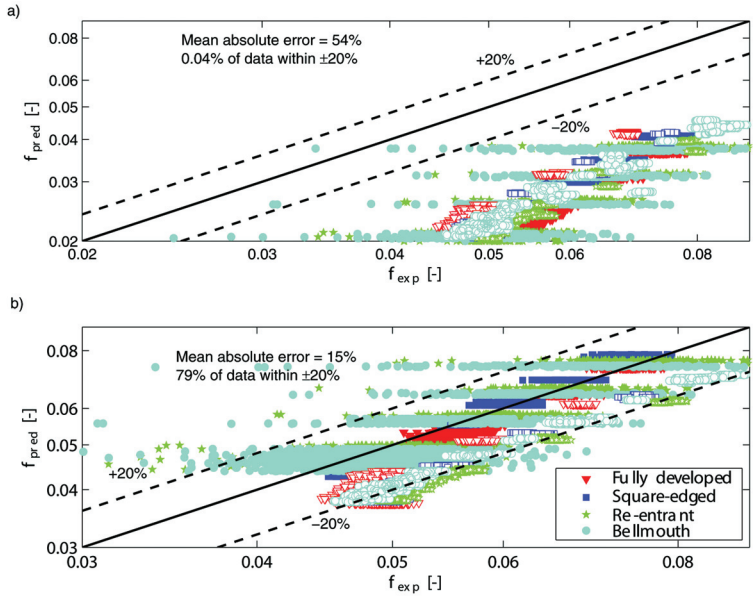

Figure 17. Diabatic friction factor data compared with Tam and Ghajar's (1997) (a) original and (b) modified correlations.

An interesting feature of the plot of the Colburn *j*-factor, however, is that the friction factor plot can be inserted on the same graph. This graph then shows the parallel behavior of *j* versus Re and *f* versus Re. This is shown in Figure 18a, with the friction factors in the top part of the graph and the Colburn *j*-factors in the bottom part.The trends of the two graphs are striking. In fact, by multiplying the *j*-factors by $4\mathrm{Pr}^{2/3}$, all the data collapse into one, as shown in Figure 18b. This is very similar to the Reynolds analogy for a flat plate and fully developed pipe flow, which is given as

$$\mathrm{StPr}^{2/3} = \frac{f}{8}, \tag{12}$$

and the extended Reynolds analogy, as given by Shah and Seculic (2003), given as

$$\mathrm{StPr}^{2/3} = \frac{f}{8}\phi_w, \tag{13}$$

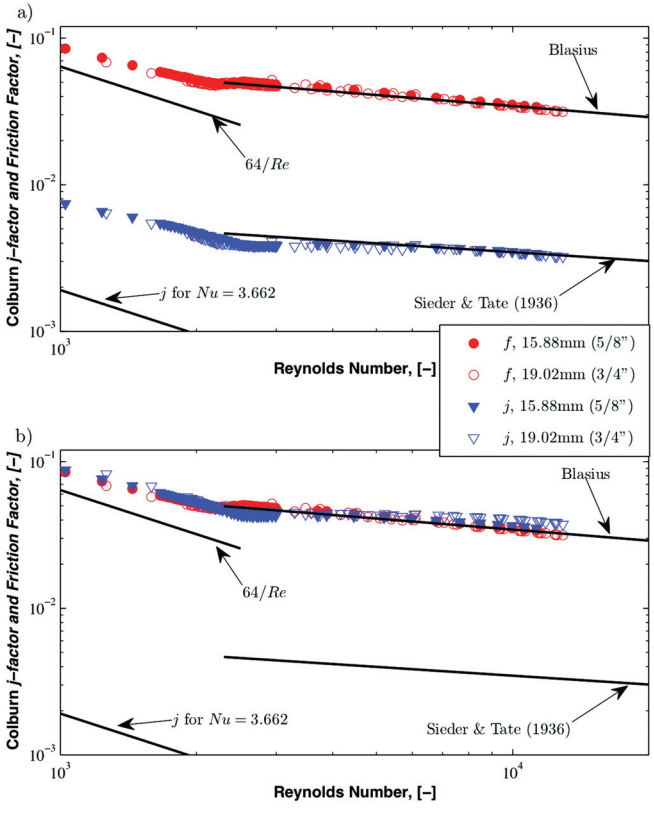

Figure 18. Correlation between friction factor and heat transfer for fully developed flow with (a) *f* and *j* versus Re and (b) *f* and $4j\mathrm{Pr}^{-2/3}$ versus Re. In (b), only the experimental data was manipulated by $4j\mathrm{Pr}^{-2/3}$.

where ϕ_w is a function of the tube/duct geometry, the flow type, boundary condition, and the Prandtl number. It, in effect, modifies the Reynolds analogy relationship between *j* and *f*. Thus, from the current experimental data, the value of ϕ_w would be $2\mathrm{Pr}^{-2/3}$, or

$$\mathrm{StPr}^{2/3} = \frac{f}{4}\mathrm{Pr}^{-2/3}. \tag{14}$$

Therefore, to predict heat transfer coefficients, only the friction factor data are needed. Likewise, if the friction factors are to be determined, only heat transfer data are required. This, however, should be seen as a special case for water in smooth tubes only, as it is bound to differ for higher Prandtl number fluids. One point that has to be mentioned is that this relation would never have been made if adiabatic friction factors were used.

To demonstrate this, the Shome and Jensen (1995) and Sieder and Tate (1936) correlations were used for the laminar and turbulent flow heat transfer models. From this, the friction factors were calculated. A plot of the predicted friction factors, according to Equation 14, with the experimental ones is shown in Figure 19. The data were predicted on average to within 8.7%, with 88% of the data being predicted to within 15%. Equation 14 is valid for $1000 < \mathrm{Re} < 15{,}000$, $3.7 < \mathrm{Pr} < 5.8$, $1 \times 10^5 < \mathrm{Gr} < 9 \times 10^5$, $0.67 < \frac{\mu}{\mu_w} < 0.87$, $0.0246 < f < 0.2092$, and $7.7 \times 10^{-4} < \mathrm{St} < 3.7 \times 10^{-3}$.

CONCLUSION

Modern water-chiller units often operate in the transition flow regime due to design or operating constraints. With the paucity of data on transition for the cooling of the fluid, designing for this regime is difficult, necessitating the current research. An experimental setup consisting of a tube-in-tube, counterflow heat exchanger, with the working fluid being water that was cooled,

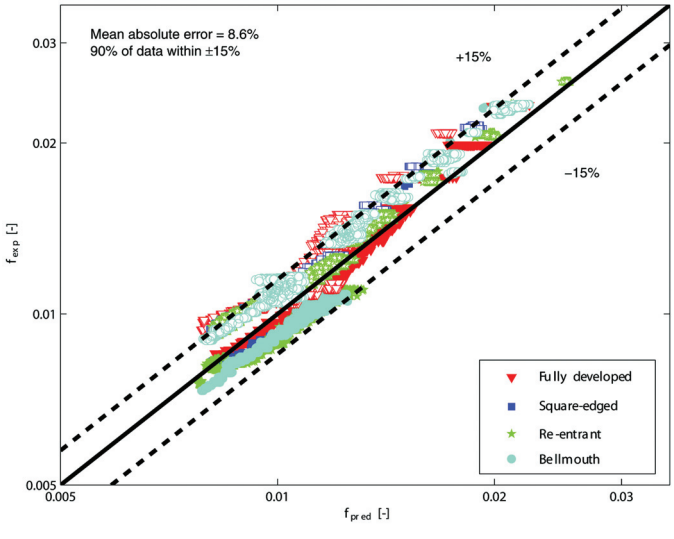

Figure 19. Performance of Equation 14 for laminar and turbulent friction factors. Solid markers denote data for the 15.88 mm (5/8 in.) tube and empty markers data for the 19.02 mm (3/4 in.) tube.

was used to obtain measurements within the transition regime. Single-phase smooth tube heat transfer and friction factor results in the transition regime were presented. The effect of tube diameter and entrance effects on the transition region of flow were investigated.

Adiabatic friction factors showed that transition from laminar to turbulent flow was strongly dependent on the type of inlet used, confirming results from another study. The smoother the inlet, the more transition was delayed. Results for the bellmouth inlet showed the largest delay, with transition only occurring at a Reynolds number of approximately 12,000. Hysteresis in the transition region was also negligible following repeated tests of increasing and decreasing the Reynolds numbers.

Heat transfer results, on the other hand, showed that transition was totally independent of the type of inlet used. This was due to the buoyancy-induced secondary flows influencing the flow, such that it dampens the effects of the inlet profiles. Laminar heat transfer results were also much higher than their theoretically predicted values, due to the secondary flows increasing the amount of mixing within the tube. Turbulent heat transfer data were unaffected by the entrance type and natural convection flows.

Diabatic friction factor results also showed that transition was independent of the type of inlet, confirming the heat transfer results. Laminar friction factors were, however, much higher than the values predicted by the Poiseuille relation. This was also attributed to the natural convection flows influencing the boundary layer to such a degree that the shear stress at the tube wall was higher than normal.

A correlation between diabatic friction factors and heat transfer coefficients in the form of a Reynolds analogy-type equation was presented. It was shown that the laminar and turbulent friction factors were predicted on average to within 8.7%, with 88% of the data being predicted to within 15%.

ACKNOWLEDGMENT

The following organizations are thanked for their support: ASHRAE, which was the main sponsor of this project (RP-1280), the University of Pretoria, the Technology and Human Resources for Industry Programme (THRIP)-AL631, the Tertiary Education Support Programme (TESP) from Eskom and the National Research Foundation and the SANERI/University of Stellenbosch Solar Hub. Dr. L. Liebenberg is thanked for being involved in the initial phase of this project as cosupervisor at the University of Pretoria.

NOMENCLATURE

A	=	area, m^2 (ft^2)
A_i	=	inner tube inside heat transfer area, m^2 (ft^2)
A_o	=	inner tube outside heat transfer area, m^2 (ft^2)
D_i	=	inner diameter of tube, m (ft)
f	=	Darcy-Weisbach friction factor
Gr	=	Grashof number
Δh_i	=	inner-tube enthalpy difference, J/kg (Btu/h)
j	=	Colburn j-factor
L	=	tube length, m (ft)
$\dot{m}_i$	=	inner-tube fluid mass flow rate, kg/s (lb/s)
$\dot{m}_o$	=	annulus fluid mass flow rate, kg/s (lb/s)
Nu	=	Nusselt number based on D_i
Pr	=	Prandtl number
Δp	=	differential pressure drop, Pa (lb_f/in^2)
$\dot{Q}_i$	=	heat transfer rate for inner-tube fluid, W (Btu/h)
Re	=	Reynolds number based on D_i
R_w	=	tube-wall resistance, K/W (°F·h/Btu)
St	=	Stanton number
T_i	=	average fluid temperature for inner tube, °C (°F)
T_o	=	average fluid temperature for annulus, °C (°F)
T_{lmtd}	=	log-mean temperature difference, °C (°F)
T_{wi}	=	temperature of fluid at inner tube inner wall, °C (°F)
T_{wo}	=	temperature of fluid at inner tube outer wall, °C (°F)
U	=	overall heat transfer coefficient, $W/m^2 \cdot K$ (Btu/h·ft^2·°F)
u	=	average fluid velocity in the inner tube, m/s (ft/s)

Greek Symbols

α_i	=	heat transfer coefficient of inner tube, W/m^2·K (Btu/h·ft^2.°F)	ϕ_w	=	variable in Equation 13
α_o	=	heat transfer coefficient of annulus, W/m^2·K (Btu/h·ft^2.°F)	μ	=	dynamic viscosity, Pa·s (lb/ft·s)
ρ	=	fluid density, kg/m^3 (lb/ft^3)	μ_w	=	dynamic viscosity at tube wall, Pa·s (lb/ft·s)

Subscripts

exp	=	experimental	*pred*	=	predicted
in	=	inner tube, inlet	Δp	=	pressure drop
hx	=	Heat transfer	*out*	=	outer tube, out

REFERENCES

Allen, R.W., and E.R.G. Eckert. 1964. Friction and heat-transfer measurements to turbulent pipe flow of water (Pr=7 and 8) at uniform wall heat flux. *Journal of Heat Transfer* 86:301–10.

ASHRAE. 2009. *2009 ASHRAE Handbook—Fundamentals*, Chapter 3. Atlanta: American Society of Heating, Refrigerating and Air-Conditioning Engineers, Inc.

Churchill, S.W. 1977. Comprehensive correlating equations for heat, mass and momentum transfer in fully developed flow in smooth tubes. *Industrial and Engineering Chemistry Fundamentals* 16:109–16.

Colburn, A.P. 1933. A method of correlating forced convection heat transfer data and a comparison with fluid friction. *Transactions of the American Institute for Chemical Engineers* 29:174–210.

Durst, F., S. Ray, B. Unsal, and O.A. Bayoumi. 2005. The development lengths of laminar pipe and channel flows. *Journal of Fluids Engineering* 127:1154–60.

Faris, G.N., and R. Viskanta. 1969. An analysis of laminar combined forced and free convection heat transfer in a horizontal tube. *International Journal of Heat and Mass Transfer* 12:1295–1309.

García, A., P.G. Vicente, and A. Viedma. 2005. Experimental study of heat transfer enhancement with wire coil inserts in laminar-transition-turbulent regimes at different Prandtl numbers. *International Journal of Heat and Mass Transfer* 48:4640–51.

Ghajar, A.J., and K.F. Madon. 1992. Pressure drop measurements in the transition region for a circular tube with three different inlet configurations. *Experimental Thermal and Fluid Science* 5:129–35.

Ghajar, A.J., and L.M. Tam. 1991. Laminar-transition-turbulent forced and mixed convective heat transfer correlations for pipe flows with different inlet configurations. *HTD, Fundamentals of Forced Convective Heat Transfer, ASME* 181:15–23.

Ghajar, A.J., and L. Tam. 1994. Heat transfer measurements and correlations in the transition region for a circular tube with three different inlet configurations. *Experimental Thermal and Fluid Science* 8:79–90.

Gnielinski, V. 1976. New equations for heat and mass transfer in turbulent pipe and channel flow. *International Chemical Engineering* 16:359–68.

Hwang, G. J., and C.W. Tsai. 1977. Theoretical and experimental studies of laminar mixed convection in water pipe flow with density inversion effect. *International Journal of Heat and Mass Transfer* 40:2019–33.

IAPWS. 2003. Uncertainties in enthalpy for the IAPWS formulation 1995 for the thermodynamic properties of ordinary water substance for general and scientific use (IAPWS-95) and the IAPWS industrial formulation 1997 for the thermodynamic properties of water and steam (IAPWS-IF97), Advisory Note No 1. International Association for the Properties of Water and Steam.

Kline, S.J., and F.A. McClintock. 1953. Describing uncertainties in single-sample experiments. *Mechanical Engineering* 75:3–8.

Koch, R. 1960. Pressure loss and heat transfer for turbulent flow. *Atomic Energy Commission Translation Series* 3875:1–135.

Lienhard, J.H., and J.H. Lienhard. 2003. *A Heat Transfer Text Book*. Cambridge: Phlogiston Press.

Manglik, R.M., and A.E. Bergles. 1993a. Heat transfer and pressure drop correlations for twisted-tape inserts in isothermal tubes: Part 1—Laminar flows. *Journal of Heat Transfer* 115:881–89.

Manglik, R.M., and A.E. Bergles. 1993b. Heat transfer and pressure drop correlations for twisted-tape inserts in isothermal tubes: Part 2—Transition and turbulent flows. *Journal of Heat Transfer* 115:890–96.

Maré, T., N. Galanis, I. Voicu, and J. Miriel. 2006. Experimental analysis of mixed convection in inclined tubes. *Applied Thermal Engineering* 26:1677–83.

Metais, B., and E.R.G. Eckert. 1964. Forced, mixed and free convection regimes. *Transactions of the ASME Journal of Heat Transfer* 10:295–96.

Mikesell, R.D. 1963. The effects of heat transfer on the flow in a horizontal pipe. PhD dissertation, Chemical Engineering Department, University of Illinois, IL.

Morel, T. 1975. Comprehensive design of axisymmetric wind tunnel contractions. *Journal of Fluids Engineering* 97:225–33.

Mori, Y., K. Futagami, S. Tokuda, and M. Nakamura. 1966. Forced convective heat transfer in uniformly heated horizontal tubes. *International Journal of Heat and Mass Transfer* 9:453–63.

Nagendra, H.R. 1973. Interaction of free and forced convection in horizontal tubes in the transition regime. *Journal of Fluid Mechanics* 57:269–88.

Nunner, W. 1956. Heat transfer and pressure drop in rough tubes. *VDI-Forschungsheft* 455-B:5-39.

Oliver, D.R. 1962. The effect of natural convection on viscous-flow heat transfer in horizontal tubes. *Chemical Engineering Science* 17:335–50.

Olivier, J.A. 2009. Single-phase heat transfer and pressure drop of water cooled at a constant wall temperature inside horizontal smooth and enhanced tubes with different inlet configurations in the transitional flow regime. PhD dissertation, Department of Mechanical and Aeronautical Engineering, University of Pretoria, South Africa.

Ou, J.W., and K.C. Cheng. 1977. Natural convection effects on Graetz problem in horizontal isothermal tubes. *International Journal of Heat and Mass Transfer* 20:953–60.

Patel, V.C., and M.R. Head. 1969. Some observations on skin friction and velocity profiles in fully developed pipe and channel flows. *Journal of Fluid Mechanics* 38:181–201.

Petukhov, B.S., A.F. Polyakov, and B.K. Strigin. 1969. Heat transfer in tubes with viscous-gravity flow. *Heat Transfer-Soviet Research* 1:24–31.

Rayle, R.E. 1959. Influence of orifice geometry on static pressure measurements. *ASME Paper No. 59-A-234.*

Senecal, V.E., and R.R. Rothfus. 1953. Transition flow of fluids in smooth tubes. *Chemical Engineering Progress* 49:533–38.

Shah, R.K. 1978. A correlation for laminar hydrodynamic entry length solutions for circular and noncircular ducts. *Journal of Fluids Engineering* 100:177–79.

Shah, R.K., and D.P. Seculic. 2003. *Fundamentals of Heat Exchanger Design*. New York: John Wiley and Sons.

Shome, B., and M.K. Jensen. 1995. Mixed convection laminar flow and heat transfer of liquids in isothermal horizontal circular ducts. *International Journal of Heat and Mass Transfer* 38:1945–56.

Sieder, E.N., and G.E. Tate. 1936. Heat transfer and pressure drop in liquids in tubes. *Industrial and Engineering Chemistry* 28:1429–35.

Siegwarth, D.P., R.D. Mikesell, T.C. Readal, and T.J. Hanratty. 1969. Effect of secondary flow on the temperature field and primary flow in a heated horizontal tube. *International Journal of Heat and Mass Transfer* 12:1535–52.

Smith, A.M.O. 1960. Remarks on transition in a round tube. *Journal of Fluid Mechanics* 7:565–76.

Tam, L., and A.J. Ghajar. 1997. Effect of inlet geometry and heating on the fully developed friction factor in the transition region of a horizontal tube. *Experimental Thermal and Fluid Science* 15:52–64.

Tam, L., and A. Ghajar. 1998. The unusual behavior of local heat transfer coefficient in a circular tube with a bell-mouth inlet. *Experimental Thermal and Fluid Science* 16:187–94.

Tam, L., and A.J. Ghajar. 2006. Transitional heat transfer in plain horizontal tubes. *Heat Transfer Engineering* 27:23–38.

Wagner, W., and A. Pruß. 2002. The IAPWS formulation 1995 for the thermodynamic properties of ordinary water substance for general and scientific use. *Journal of Physical and Chemical Reference Data* 31:387–535.

White, F.M. 1991. *Viscous Fluid Flow*. Singapore: McGraw Hill.